Chemical Science International Journal

29(5): 32-50, 2020; Article no.CSIJ.58808
ISSN: 2456-706X
(Past name: American Chemical Science Journal, Past ISSN: 2249-0205)

Biosorption of Bromophenol Blue from Aqueous Solution Using Flamboyant (*Delonix regia)* Pod

Ebenezer Olujimi Dada[1,2], Ilesanmi Ademola Ojo[1,2], Abass Olanrewaju Alade[1,2,3*], Tinuade Jolaade Afolabi[1,2], Omotayo Sharafdeen Amuda[4] and Ahmad Tariq Jameel[5]

[1]Department of Chemical Engineering, Ladoke Akintola University of Technology (LAUTECH), Ogbomoso, Nigeria.
[2]Bioenvironmental, Water and Engineering Research Group, (BWERG), Ladoke Akintola University of Technology, Ogbomoso, Nigeria.
[3]Science and Engineering Research Group, (SEARG), Ladoke Akintola University of Technology, Ogbomoso, Nigeria.
[4]Department of Pure and Applied Chemistry, Ladoke Akintola University of Technology, Ogbomoso, Nigeria.
[5]Biotechnology Engineering Department, International Islamic University, Kuala Lumpur, Malaysia.

Authors' contributions

This work was carried out in collaboration among all the authors. Authors EOD, AOA and TJA jointly designed the study. Author OSA wrote the protocol while author AOA wrote the first draft of the manuscript. All authors managed the analyses of the study. Authors IAO and ATJ managed the literature searches. All authors read and approved the final manuscript.

Article Information

DOI: 10.9734/CSJI/2020/v29i530179
Editor(s):
(1) Dr. Thomas P. West, Texas A&M University, USA.
Reviewers:
(1) Naveen Kumar Reddy Bogireddy, Universidad Autónoma del Estado de Morelos (UAEM), México.
(2) Febiyanto, Universitas Gadjah Mada Yogyakarta, Indonesia.
Complete Peer review History: http://www.sdiarticle4.com/review-history/58808

Original Research Article

Received 28 April 2020
Accepted 03 July 2020
Published 18 July 2020

ABSTRACT

Matured flamboyant pods (FBP) activated with $ZnCl_2$ were used for batch adsorption of Bromophenol blue (BPB) dye under the effects of concentration (10-200 ppm), contact time (20-300 min), biosorbent dosage (20-120 mg) and particle size (300-850 µm). The data obtained were fitted to Langmuir and Freundlich isotherm models as well as pseudo-first-order (PFO), pseudo-second-order (PSO) and Elovich kinetic models. The highest adsorption capacity and removal

**Corresponding author: E-mail: aoalade@lautech.edu.ng*

efficiency of 7.5762 mg/g and 75.76%, respectively, were obtained under the effects of initial dye concentrations. The correlation coefficient (R^2) for the Langmuir and Freundlich isotherms are in the range 0.9938-0.9979 and 0.9895-0.9953, respectively, while, R^2, in the ranges 0.5931-0.815, 0.9962-1.000 and 0.8046-0.8828, were obtained for the PFO, PSO, and Elovich kinetic models, respectively. The order of fit of the kinetic models is PSO > Elovich > PFO. The study suggests flamboyant pod as promising biomass for the remediation of dye-bearing industrial effluents.

Keywords: Biosorbent; biosorption; bromophenol blue; Delonix regia; dye.

1. INTRODUCTION

Anthropogenic activities have caused great harm to the quality of life in the terrestrial and aquatic environments [1]. Specifically, the generation of wastewater from various industrial activities depletes the quality of freshwater resources considerably and dyes have been marked as important pollutants among the organic pollutants that are recalcitrant in the environment [2]. Dyes are coloured substances that have affinity to the substrate to which they are applied. Dyes' colourations are due to their ability to absorb some wavelengths of light more than other substances [3,4].

Many industries such as textile, leather, paper, printing, plastic, and so on generate large amount of wastewater containing dyes. Dyes present in water designated to be treated in municipal water treatment operations are difficult to treat due to the complicated chemical structures and high visibility of these dyes [5]. Colour displayed by dyes in most water bodies makes such water unpleasant, while the level of concentration and exposure can manifest acute or chronic effects on exposed organisms [6,7]. However, some of the dyes have been classified as being toxic and even carcinogenic [8,9].

Some of the several techniques for the removal of dyes from wastewater include flotation, precipitation, oxidation, filtration, coagulation, ozonation and biological process. Meanwhile, biosorption process, which is an environmental-friendly method, has been deployed as a promising process for the removal of dyes from effluent [10]. The biosorption process is an effective alternative method to the conventional methods, which are characterised by high cost and other complicated operations [11,12]. The process is similar to the adsorption process which involve uptake of toxic substances by biomass from contaminated fluid stream.

Activated carbon is the most widely used adsorbent for the effective removal of dyes, due to its large surface area, microporous structure, and high adsorption capacity among others [13]. However, its usage in large-scale treatment process is very limited due its high cost of production and this has led to the desire for materials that are cost-effective, efficient, and easily available for the production of the adsorbents [14]. Some of the proven efficiently adsorbent materials are peanut hull [15], orange and banana peels [16], pumpkin seed hull [17], and *Posidonia oceanica* (L.) fibre [18].

The biosorption method has proved to be an excellent way of treating industrial waste effluents, offering significant advantages like low-cost, availability, profitability, easy operation, and efficiency. Several researchers had used agricultural wastes to sequester potentially toxic elements from wastewater [19].

Flamboyant is a perennial plant with fast growth up to 10-15 m height. Its branches spread like an umbrella, providing shade beneath the parent tress and as such, it has become one of the important and widely cultivated ornamental trees grown in the tropics and some other parts of the world [20]. Flamboyant is characterised with corymbs, 15-30 cm long, and bear five equal petals fragrant flowers [21]. The corymbs matured, after fertilisation, to produce, strap-shaped and flattened pod (30-70 cm long), which houses about 50 leguminous seeds. The initially leathery pods, developed into reddish-brown or black and woody, when ripe [21]. The matured pod sheds after ripen and litter the vicinities of the parent trees. Small quantity of the woody pod is used as solid fuel in some rural areas, while the remaining are burnt or left to litter the host environment, with untidy outlook [22].

This development has led to challenges of solid waste disposal in most developing nations such as Nigeria, where the population of the flamboyant tree is high. This development has necessitated the conversion of these wastes to useful and value-added products, such as adsorbent that possess the potential of

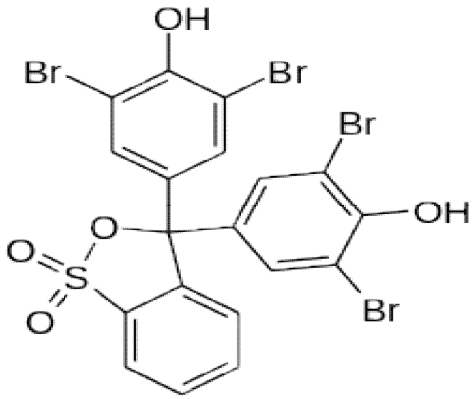

Fig. 1. Structure of bromophenol blue dye

amelioration other environmental challenges such as water pollution [21]. Flamboyant pods have been prepared and characterised as adsorbent for the remediation of wastewater containing various organic and inorganic pollutants [20]. Pandimadevi, et al. [23]; Mithun, et al. [24]; Adebisi, et al. [25]; Syed, et al. [26]; Owoyokun, et al. [27]; Alade, et al. [20]; Sugumaran, et al. [28]; and Jimoh, et al. [29] have deployed activated carbon or biosorbent derived from the flamboyant pod for the removal of dyes (methylene blue, aniline blue), heavy metals (Hg, Co, Cu, and Pb) and organic pollutants (naphthalene) from synthetic wastewaters.

Bromophenol blue is an organic chemical compound formed from the addition of excess bromine and hot solution of phenolsulfonphthalein in glacial acetic acid. It is largely used as a pH indicator, an electrophoretic colour marker and an industrial dye [12].

The chemical formula, molar mass, boiling and melting point of Bromophenol blue is $C_{19}H_{10}Br_4O_5S$ (Fig. 1) 669.96 $gmol^{-1}$, 279°C (534°F) and 273°C (523°F), respectively, while its absorbance is exhibited at maximum wavelength of 206, 283 and 424 nm [30]. The dye's apparent colour shifts depend on the concentration and/or path length through which the solution is observed and this gives the dye its dichromatic colour characteristics. Bromophenol blue is one of the dye substances with the highest value of Kreft's dichromaticity index and this indicates that changes in its colour hues depends on the changes in the thickness or concentration of the observed sample [30].

Various studies on the removal of Bromophenol Blue dye from aqueous solution include the use of acid-activated clay, *Gelidium cartilagineum* powder, Bentonite carbon composite material and UV-radiation with ZnO as a catalyst, have been reported by Okoye, et al. [31], Ch, et al. [32], El-Dars, et al. [33], and Mashkour, [34], respectively, but the efficacy of the flamboyant pod as biomass for the removal of Bromophenol blue has not been reported, thus this study was set up to demonstrate the effectiveness of these abundant materials for the removal Bromophenol blue from aqueous solutions. The study was conducted in batch and necessary adsorption properties such as isotherms and kinetic models were investigated to evaluate the efficacy of the agricultural precursor in the treatment of aqueous solution containing Bromophenol blue dye.

2. MATERIALS AND METHODS

2.1 Material and Reagents

The basic material used for this study were matured Flamboyant pods (FBPs) that were found littering the vicinity of the parent trees in Mandate Area, Ilorin, Kwara State, Nigeria. Some of the reagents used are distilled water, zinc chloride ($ZnCl_2$), bromophenol blue (BPB) tetraoxosulphate (VI) acid (H_2SO_4) and Sodium hydroxide (NaOH). These reagents were of analytical grades and were used without further purification.

2.2 Experimental Methods

2.2.1 Materials preparation

The raw FBPs were cut into pieces (3-4 cm), washed with tap water, and rinsed thoroughly with distilled water to remove any soluble materials attached to the FBP surface [35]. They were then dried to constant weight before being

ground to smaller sizes in a mill and then sieved to obtain three different mesh particle sizes (850 µm, 425 µm, and 300 µm).

2.2.2 Activation with zinc chloride

Zinc Chloride solution (0.1 M) was prepared by dissolving 13.63 g of $ZnCl_2$ in 1 L distilled water. The dried flamboyant particle mixed with zinc chloride solution in a ratio of 3:5 (w/v). The mixture was kept at room temperature for 24 h and later boiled off in the Fume cupboard until it formed paste [20]. The mixture was allowed to cool and then washed with distilled water to remove excess reagent until the pH was stable between 6.9 and 7.1. The mixture was filtered and the residue, which is now the Activated Flamboyant Pod (AFBP), was oven-dried at 105°C to constant weight and kept for further use [20].

2.3 Characterization

2.3.1 Moisture content determination

The FBP sample (0.1 g) was placed in a pre-weighed sample container and then charged into an oven at 105°C for 24 h [36,37]. The sample was then removed and cooled in a desiccator, before being re-weighed. The amount of moisture removed was evaluated using Eq. (1) [38].

$$Moisture\ content = \frac{M_i - M_f}{M_i}\ X\ 100\% \quad (1)$$

where, m_i = Mass of the initial sample and m_f = Mass of the final sample after drying

2.3.2 Determination of ash content

The FBP sample (2.5 g) was put in a pre-weighed porcelain crucible and then charged into a muffle furnace at 760°C for 90 mins for the samples to turn to ashes [39]. The crucibles were collected, after the required heating, and cooled in a desiccator and then weighed. The amount of ash was deduced according to Eq. (2).

$$\%\ Ash\ = \left[\frac{Weight\ of\ sample\ remaining}{Weight\ of\ original\ sample}\right] X\ 100\% \quad (2)$$

2.3.3 Determination of volatile matter

The volatile matter was determined by taking 1.5 g of the FBP sample in a silica crucible with a porous silica cover and then heated for 7 min at a constant temperature of 925°C in a furnace. The crucible was collected and cooled in a desiccator then re-weighed [40]. The amount of volatile matter present in the sample was given as the difference in the masses of the crucibles before and after heating [23].

2.3.4 Determination of fixed carbon

The fixed carbon (F.C.) represents the carbon content in a sample that has not combined with any other element (in a free state). The amount of fixed carbon in the FBP sample was computed by deducting the sum of the percentage of ash, moisture, and volatile matter content of FBP from a hundred percent as expressed in Eq. (3) [41].

$$Fixed\ carbon\ = 100 - (moisture\ \% + ash\ \% + volatile\ matter\ \% \quad (3)$$

2.3.5 Surface characteristic

Fourier Transform Infrared Spectroscopy (FTIR) was employed to study the surface chemistry of both raw and activated FBP samples [42,43]. This will identify the main chemistry that could be responsible for the adsorption process. The spectrum of the biosorbent was within the range of 400-4000 cm^{-1} wave number. The comparison of the FTIR spectra of the FBP and AFBP was done.

2.4 Preparation of Stock Solution of Bromophenol Blue (BPB) Dye

BPB dye stock solution was prepared by dissolving 1.0 g of BPB dye powder in 1.0 L of distilled water. Different concentrations such as 5, 10, 15, 20, 25, and 30 mg/L of the solution were prepared via appropriate dilution [44]. The absorbance of each dye concentration was recorded at 590 nm using UV/Vis spectrophotometer and the values obtained were used to develop the absorbance-concentration profile as the calibration curve used in this study [45].

2.5 Batch Adsorption Studies

Batch adsorption experiments for the removal of BPB using the activated FBP biosorbent were performed at selected contact time (10-270 min), initial concentration (5-30 mg/L), biosorbent dosage (100-700 mg) and particle sizes (300-850 µm) of the biosorbent. The required amount of the AFBP was added to 100 ml of different concentrations of BPB solutions and then agitated at pre-set speed (rpm). The dye solution

was then decanted and centrifuged at 1,500 rpm for 30 min and the absorbance of the supernatant was then analysed using a UV-Vis spectrophotometer at 590 nm [46]. The unabsorbed amount of the BPB was quantified accordingly. Adsorption capacity and percentage removal were then determined accordingly Eq. (4-5) [31].

$$q_e = \frac{V(C_o - C_e)}{W} \quad (4)$$

$$Removal\ (\%) = \frac{(C_o - C_e)}{C_o} X100 \quad (5)$$

where, V is the volume (L) of dye solution used; C_o and C_e are initial and final concentrations of the BPB dye in solution (mg/L), W is the amount (g) of AFBP used [33].

2.5.1 Effect of initial dye concentration

The effect of initial dye concentration (5-30 mg/L) on adsorption of BPB was studied by mixing 300 mg of FBP in a 250 ml flask containing 100 ml of the desired dye solution at room temperature and agitated at 200 rpm for 1 h [34,47]. The dye solution was then decanted and centrifuged at 1,500 rpm for 30 min and the absorbance of the supernatant was then analysed using a UV-Vis spectrophotometer at 590 nm [46]. The unabsorbed amount of the BPB was quantified accordingly.

2.5.2 Effect of contact time

The effect of contact time (10-270 min) was studied by mixing 100 ml of the BPB solution with 300 mg of the AFBP in different 250 ml conical flask [48]. Each flask was withdrawn from the shaker, at a pre-set time and the dye solution was decanted, centrifuged at 1,500 rpm for 30 min and the absorbance of the supernatant was analysed using UV-Vis spectrophotometer at 590 nm [46]. The unabsorbed amount of the BPB was quantified accordingly.

2.5.3 Effect of biosorbent dosage

The effect of AFBP dosage on the removal of BPB from the aqueous solution was studied by adding different dosages (100 to 700 mg) of the AFBP to 100 ml of 20 mg/L BPB dye solution in 250 ml flask at room temperature. The mixture was agitated on the rotary shaker at 200 rpm for 1 h. The dye solution was then decanted and centrifuged at 1,500 rpm for 30 min and the absorbance of the supernatant was analysed using a UV-Vis spectrophotometer at 590 nm [46]. The unabsorbed amount of the BPB was quantified accordingly.

2.5.4 Effect of particle size

Each adsorption experiment was conducted using 850 µm, 425 µm, and 300 µm particle size of the AFBP to evaluate the effect of particle size on its biosorption efficiency of AFBP for the removal of BPB. The mixture was agitated with 300 mg of each sample, at 200 rpm for 1 h. The dye solution was then decanted and centrifuged at 1,500 rpm for 30 min and the absorbance of the supernatant was then analysed using a UV-Vis spectrophotometer at 590 nm [46,49]. The unabsorbed amount of the BPB was quantified accordingly.

2.6 Biosorption Isotherms

Langmuir and Freundlich isotherm models were used to describe the biosorption isotherm of BPB from aqueous solution by the FBP developed. These isotherms were fitted to the adsorption data and the correlation coefficient, (R^2) was used to express the fitness of the experimental data, while the model parameters were evaluated accordingly [50].

2.6.1 Langmuir isotherm

The Langmuir model is represented, commonly, as in Eq. (6) and its linear form in Eq. (7). The Langmuir isotherm constants, b, and q_{max} were determined from the plot of $1/q_e$ versus $1/C_e$ [51].

$$q_e = (q_m K_m C_e)/((1 + K_L C_e \quad (6)$$

$$C_e/q_e = C_e/q_m + 1/K_L q_m \quad (7)$$

where, q_e = Amount of BPB adsorbed at equilibrium (mg/g), q_{max} = Maximum AFBP biosorption capacity (mg/g), b = Langmuir equilibrium constant (L/mg) and C_e = Equilibrium dye concentration in the solution (mg/L)

2.6.1.1 Separation factor

The Separation factor (R_L) is a dimensionless constant (Eq. 8) that is incorporated as an important feature in the study of Langmuir isotherm [51]. It is employed to determine the extent of satisfactoriness or otherwise in a batch adsorption system under investigation. Thus, if R_L > 1 then the isotherm is unfavourable, R_L = 1 then the isotherm is linear, R_L = 0 then the

isotherm is irreversible, while the condition of 0 < R_L < 1 indicates that the isotherm is favourable.

$$R_L = 1/(1 + bC_e) \quad (8)$$

where R_L is the separation factor, b, the constant from Langmuir equation, and C_e the initial dye concentration.

2.6.2 Freundlich isotherm

The Freundlich isotherm assumes that the adsorbent surface involved in adsorption study is heterogeneous with its adsorption sites at varying energy levels [52]. Freundlich isotherm model (Eq. 9) was investigated to determine its suitability in understanding the biosorption of BPB onto the AFBP developed. Its linear form is represented as Eq. (10), while the Freundlich isotherm constants, K_f and 1/n, were determined from the plot of log q_e versus log C_e.

$$q_e = K_f\, C_e^{1/n} \quad (9)$$

$$Log\, q_e = log\, K_f + 1/n\ log\, C_e \quad (10)$$

where, q_e = Amount of sorbate absorbed at equilibrium (mg/g), K_f = Freundlich constant ((mg/g) (L/mg) 1/n), 1/n = Freundlich exponent (dimensionless), C_e = Equilibrium dye concentration in the solution (mg/L) [52].

2.7 Biosorption Kinetic Modelling

The sorption kinetics is an important property, which is used to understand the pattern and mechanism of the adsorption process. Common kinetic models include the pseudo-first-order, pseudo-second-order kinetic, and Elovich models [50].

2.7.1 Pseudo-first-order model

The pseudo-first-order (PFO) model is described as in Eq. (11) which is usually integrated with the initial condition that q_t = 0 at t = 0 and its simplification leads to a linear form stated in Eq. (12). The Pseudo-first-order constants, k_1, and q_e, were evaluated from the plot of ln (q_e-q_t) versus t.

$$dq_t/d_t = K_1\,(q_e - q_t) \quad (11)$$

$$In\,(q_e - q_t) = Inq_e - K_1 t \quad (12)$$

where, q_e = Amount of solute absorbed at equilibrium (mg/g), q_t = Amount of solute absorbed at time t (mg/g), k_1 = Pseudo-first-order equilibrium rate constant (1/min) and t = Contact time (min)

2.7.2 Pseudo-second-order model

The pseudo-second-order (PSO) model is expressed as in Eq. (13) and can be integrated with boundary conditions t = 0 to t = t and q_t = 0 to q_t = q_t. Simplifying the integration further led to a linear form (Eq. 14) which facilitate a linear plot of t/q_t versus t to evaluate the Pseudo-second-order constants (k_2 and q_e,).

$$dq_t/d_t = K_2\,(q_e - q_t)^2 \quad (13)$$

$$t/q_t = 1/K_2 q_e^2 + t/q_e \quad (14)$$

where, q_e = Amount of solute absorbed at equilibrium (mg/g), q_t = Amount of solute absorbed at time t (mg/g), k_2 = Pseudo-second-order equilibrium rate constant (g/mg/min), t = Contact time (min)

2.7.3 Elovich model

The Elovich model equation is given as expressed in Eq. (15) and its linear form is given by Eq. (16). The Elovich coefficients such as initial adsorption rate (α), and the desorption constant (β) were evaluated from the intercept and slope of the straight-line plots of q_t against ln t [53].

$$dq_t/d_t = \alpha\, exp\,(-\beta q_t) \quad (15)$$

$$q_t = \frac{1}{\beta}\,(ln\,\alpha\,\beta) + \frac{1}{\beta}\,(ln\,t) \quad (16)$$

where α is the initial adsorption rate (mg/g min), β is related to the extent of surface coverage and activation energy for chemisorption (g/mg).

2.8 Test of Kinetics Model

The suitability of PFO and PSO, to provide insight into the adsorption mechanism that took place between the AFBP developed and the BPB dye in aqueous medium was verified with one of the common error analyses such as the Sum of Error Squares (SSE, %) stated in Eq. (17) [54].

$$\%\,SSE = \sqrt{\left(\frac{\sum\left[(q_{e(exp)} - q_{e(cal)})^2\right]}{N}\right)} \quad (17)$$

where $q_{e(exp)}$ = Adsorption capacity at equilibrium experimental (mg/g), $q_{e(cal)}$ = Adsorption capacity

at equilibrium calculated (mg/g) and N = Number of data point.

3. RESULTS AND DISCUSSION

3.1 Characteristics of AFBP Developed

The proximate analysis of the biosorbent expressed in terms of moisture content, ash content, volatile matter, and fixed carbons, (Table 1) indicate that ash content of treated flamboyant pods was 31.20%, which is lower than the ash content (33.85%) of the untreated FBP. Low ash content is often preferred for effective adsorbent [50]. The lower ash content suggests that the AFBP has improved and better sorbent properties that the untreated. It further indicates that the activation process has improved the property of the raw FBP. However, the ash content (33.85% and 31.20%) observed for untreated and treated FBPs in this study, were higher than 2.80%, 12.87% and 15.73% reported by Seshadri, et al. [37] and Pandimadevi, et al. [23] (Table 1). This development may be attributed to the variations in the composition of different species of flamboyant trees in different regions of the world.

The moisture content of AFBP, 9.90% is much higher than that of FBP, 3.66% and these values are higher than 0.22% reported by Seshadri, et al. [37] while only the moisture content of the treated flamboyant pods is higher than 5.21% reported by Pandimadevi, et al. [23]. This increase may be due to the treatment processes, particularly, activation where the material was soaked in the activants for a long time and the drying process involved in the study was to constant weight and not to complete dryness.

The fixed carbon (24.90%) of treated flamboyant pods is much higher than that (14.85%) of untreated flamboyant pods and this suggests that it would be more economical to choose AFBP flamboyant pods as the precursor of biosorbent production. The fixed carbon 14.85% and 24.90% for FBP and AFBP, respectively, are higher than 5.20%, 5.95%, 7.40% and 8.30% reported by Seshadri, et al. [37], Hesas, et al. [55], Ponnusami, et al. [56] and Pandimadevi, et al. [23], respectively. The volatile matter (47.64% and 34.00%) observed for FBP and AFBP in this study, were less than 92.03% and 75.97% reported by Seshadri, et al. [37] and Pandimadevi, et al. [23], respectively. This indicates that the volatile matter of the species of flamboyant used in this study is relatively different from the species used in previous studies [52], although not stated.

3.2 Fourier transforms Infrared Spectroscope (FTIR) Analysis

The FTIR spectra of both FBP and AFBP biosorbent are shown in Fig. 2a-b. The spectrum of the biosorbent was measured within the range of 400-4000 cm^{-1} wave number. The spectrum of FBP before activation with $ZnCl_2$ showed prominent peaks at 3495.3 cm^{-1} and 2954.6 cm^{-1} (Fig. 2a) that are attributed to O–H stretching and C-H stretching bond of alkyl group respectively. A small peak was noticed at about 2011.0 cm^{-1} and assigned to the C–H stretching vibration of an alkyl group, and the band at 1710.9 cm^{-1} is related to the C=O stretching carbonyl group, another band was found at about 1117.5 cm^{-1}, which is ascribed to C=C stretching alkenes group. The sharp peak at 2500 cm^{-1} is assigned to O–H stretching bond which is found in the chemical structure of BPB (Fig. 1, above).

Some of the peaks observed in FBP spectra were still present in AFBP after treated with $ZnCl_2$, however, there were some changes in their wave numbers (Fig. 2b), indicating that the activant have interacted chemically with the flamboyant pod sample. The prominent peak that appeared at about 3495.3 cm^{-1} was reduced to 3485.7 cm^{-1} and the peak of the C-H stretching alkyl group decreased from 1710.9 cm^{-1} to 1710.1 cm^{-1}. The peak 1117.5 cm^{-1} of the C=C band decreased to 1101.0 cm^{-1} which is an indication that a new peak has been formed and it is related to N-H bending of amide group. This is predicting that the functional groups have responsibility for the electrostatic attraction of zinc chloride cations onto flamboyant pod powder [57].

3.3 Effect of Various Parameters on Removal of Bromophenol Blue Dye

3.3.1 Effect of initial dye concentrations on biosorption

The changes in adsorption capacity and percentage removal with varying initial concentration (Fig. 3a-b), respectively, indicate that the highest adsorption capacity of 7.5762 mg/g and highest removal efficiency of 75.76% were observed at the higher concentration of 30.0 mg/L while their lowest values 0.7458 mg/g and 44.7458% were recorded at 5 mg/L. Thus, the adsorption capacity and percentage removal

of the AFBP increased as the concentration of BPB increased as expected of the adsorbent [50].

Previous research has shown that increase in initial concentration influences biosorption capacity (q_e) higher qe and the works of Senthilkumar, et al. [58], as well as Murali and Uma, [59], have reported a similar trend. The actual amount of bromophenol blue dye adsorbed per unit mass of biosorbent increased with an increase in dye concentration. This phenomenon can be explained in terms of available active sites. It may be suggested that the initial concentration of BPB provided substantial during force which effectively overcomes mass transfer resistance of the dye solute between the solids and aqueous phase. Thus, at higher initial concentrations, there is a high density of BPB on the surface of AFBP and this led to high adsorption tendency [60,61].

3.3.2 Effect of contact time on biosorption

The maximum adsorption capacity obtained for 5, 10, 15, 20, 25 and 30 mg/L of BPB were 0.79, 2.28, 3.58, 4.94, 6.31 and 7.89 mg/g, respectively (Fig. 4a). The corresponding maximum removal efficiency were 47.80%, 68.31%, 71.64%, 74.15%, 75.66% and 78.42% as the time increased from 10 to 270 min (Fig. 4b).

The extent of dye removed by AFBP increased with the increased contact time. This trend was rapid at the initial period of contact and then become slower with the increasing contact time. This may be due to the strong attractive forces between the dye molecules and the biosorbent at the beginning [62], where the active sites were not occupied. However, the trend became slower due to less available sites, thus at a later time, the rate of adsorption became slower with increasing time.

Table 1. Comparison of the proximate analysis of present work to past work

Biosorbent	Moisture content (%)	Ash content (wt. %)	Volatile matter (wt. %)	Fixed carbon (%)	References
Flamboyant Pods	0.22	2.80	92.03	5.20	[37]
Flamboyant Pods	5.21	12.87	75.97	5.95	[23]
FBP	3.66	33.85	47.64	14.85	This study
AFBP	9.90	31.20	34.00	24.90	This study

FBP Flamboyant Pods, AFBP Activated Flamboyant Pods

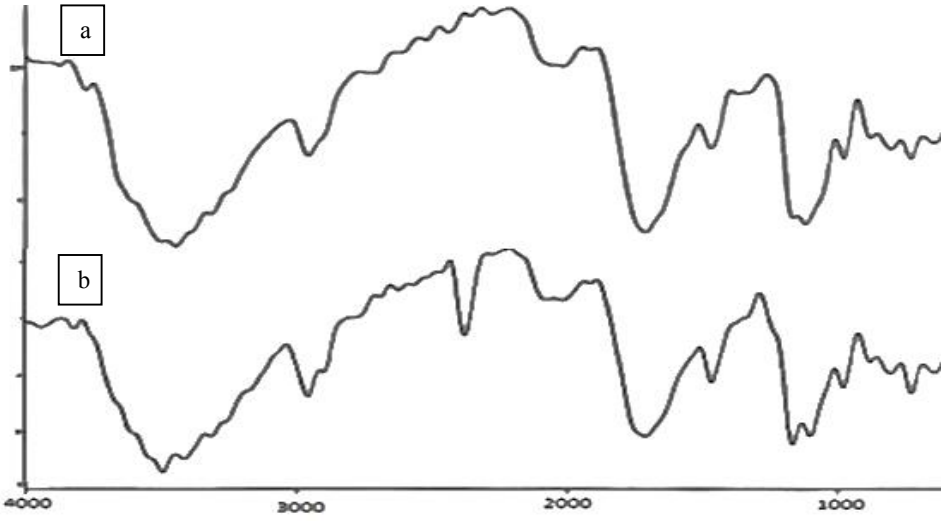

Fig. 2. FTIR spectra of (a) untreated and (b) treated flamboyant pods

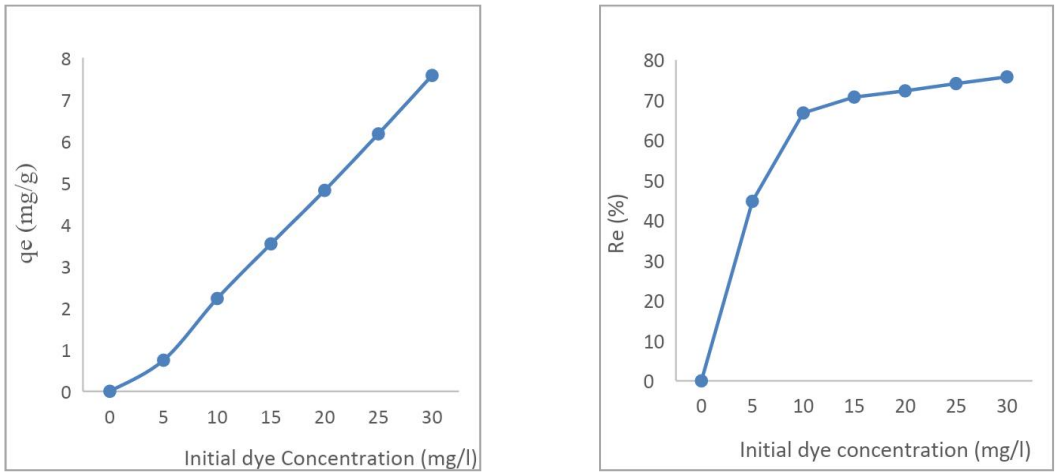

A B

Fig. 3. Plot of (a) Adsorption capacity and (b) Removal efficiency against initial dye concentration

The changes in the rate of removal with time might be because all the biosorbent sites were vacant, initially, and the solute concentration gradient was high [63]. A similar trend was reported by Khalifa, et al. [64] and Pandimadevi, et al. [23] for the adsorption of methylene blue onto jute fibre carbon. Theoretically, during adsorption, the dye molecules will move to the boundary layer of the adsorbent, initially, before diffusing into the adsorbent surface and subsequently, into the porous structure of the adsorbent. This phenomenon represents the rapid, moderate, and slow regimes displayed in this study [65].

3.3.3 Effect of biosorbent dosage on biosorption

The effect of biosorbent dosage (0.1-0.7 g) on the adsorption capacity and removal efficiency of the AFBP for removal of BPB from aqueous solution indicates that the highest adsorption capacity and removal efficiencies were 6.09 mg/g and 87.20%, respectively. The adsorption capacity of AFBP for removal of BPB increases with increasing biosorbent loading from 0.1-0.5 g (Fig. 5a-b). Certainly, the total number of active sites increased with increasing biosorbent dosage and this influenced the adsorption trend, positively. The amount of BPB adsorbed per unit mass of AFPB decreased from 6.09 to 2.49 mg/g as the dosage increased, due to a decrease in the solute transfer rate onto the surface of the adsorbent and availability of more active sites [57].

3.3.4 Effect of particle size on biosorption

Available surface area is an important controlling parameter in the biosorption process and it is inversely related to the particle size of a given biosorbent. The removal efficiency (54.90, 72.71 and 86.70%) of BPB increased with decrease in particle size (850, 425, and 300 µm) of AFBP (Fig. 6). This is because smaller particles have more surface area and this provides access for more pores in the particles. Similarly, the breaking up of large particles to form smaller ones opens some tiny sealed channels, which might then be available for adsorption process. Consequently, the sorption is often higher in adsorbent with smaller particle sizes than those with larger particle sizes. These findings are consistent with the reports of Asfaram, et al. [66] and Wanyonyi, et al. [67] for the removal of Direct Red 12B using Garlic peel and Congo Red on *E. Crassipe* roots, respectively. This relationship supports the choice of powdered adsorbent over granulated one in some adsorption studies.

3.4 Isotherm Parameters for Biosorption of BPB onto AFBP

The biosorption isotherm of BPB removal with AFBP at different initial dye concentrations was studied using the Langmuir and Freundlich models (Fig. 7a-b). The monolayer capacity q_m obtained from the plot of Langmuir isotherms (Fig. 7a) are 1.2092, 2.1730, 3.0684, 4.0933, and 5.3079 mg/g for 10, 15, 20, 25 and 30 mg/L concentration (Table 2). Langmuir constant b and

q_{max} are 0.4636-0.6559 and 1.2092-5.3079, respectively, while the Freundlich constant K_f and 1/n were in the range 4.7973-15.5382 and 0.3631-0.6387, respectively.

The overall trend obtained for the Langmuir separation factor, R_L, and the Freundlich exponent (1/n), are below one for all the concentration ranges studied, representing favourable adsorption processes, as observed for methylene blue and brilliant green dyes removal from aqueous solution with agricultural wastes activated carbon [68]. This showed good linearity for the Langmuir and Freundlich isotherm, constants are valid and this supports the applicability of the isotherms. A similar observation was reported for the adsorption of malachite green on degreased coffee beans [69].

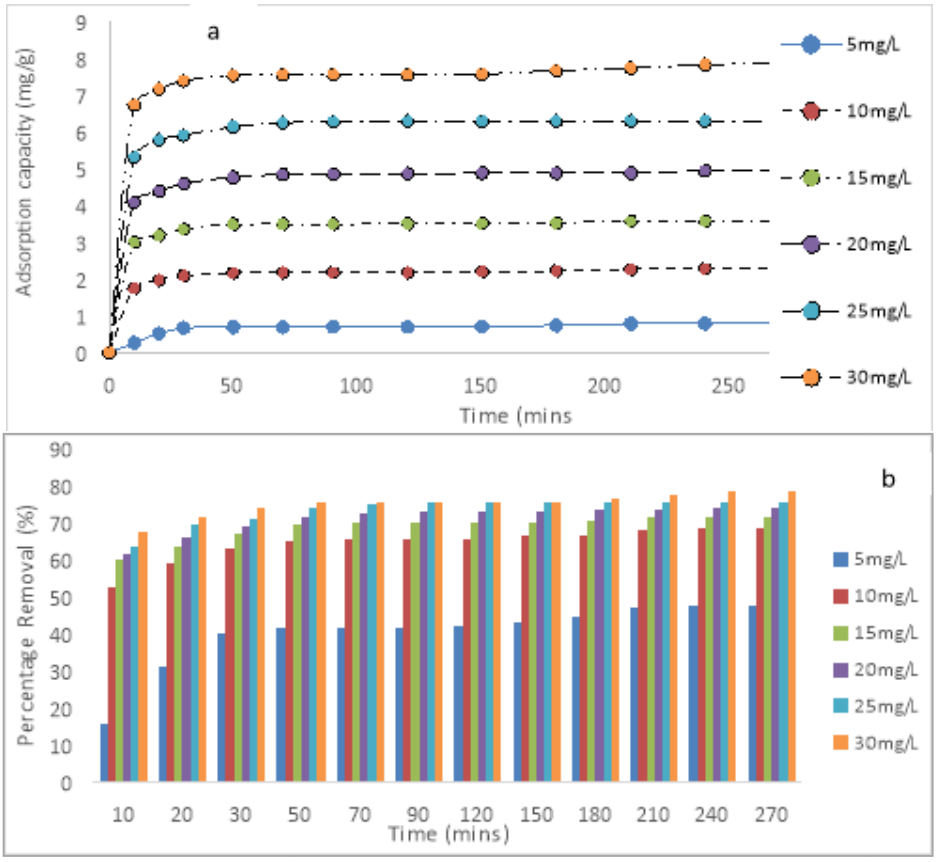

Fig. 4. Plot of (a) adsorption capacity and (b) removal efficiency against time

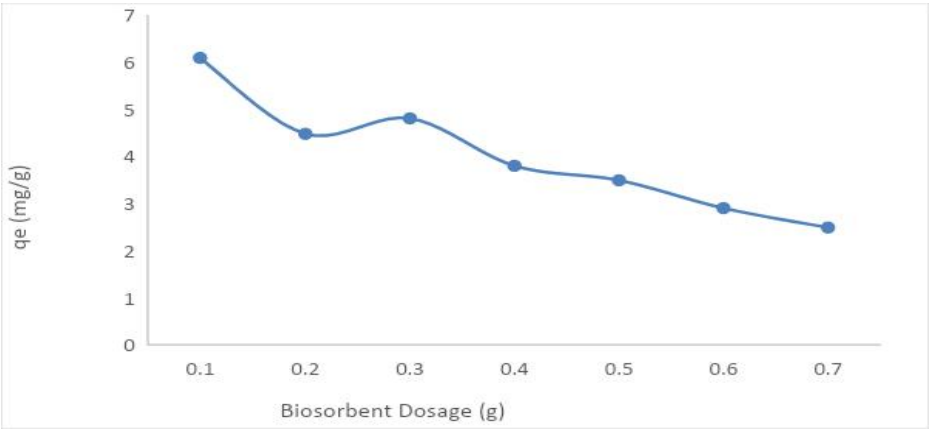

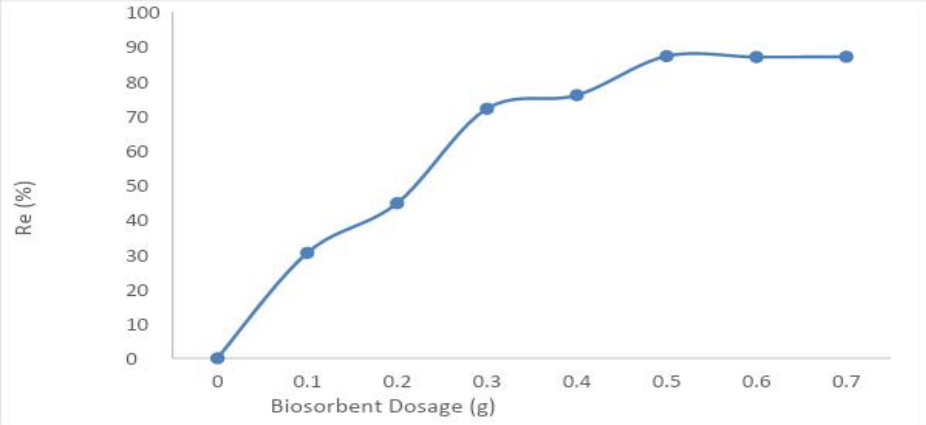

Fig. 5. Graph of (a) adsorption capacity and (b) removal efficiency against biosorbent dosage

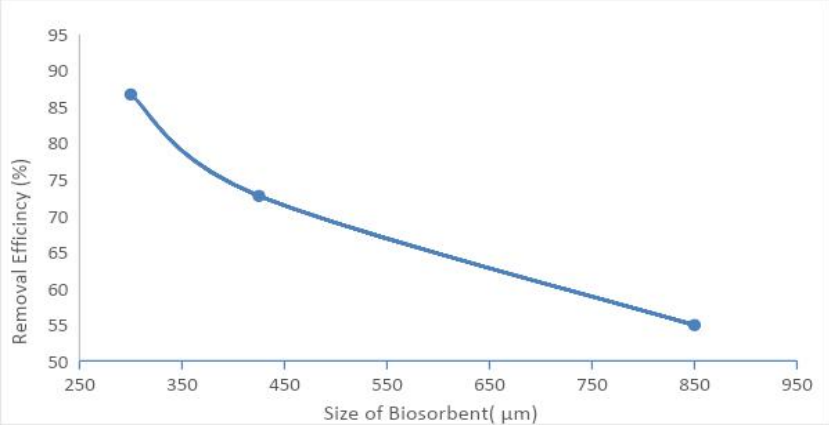

Fig. 6. Graph of particle size effect of AFBP on the removal of BPB

Table 2. Langmuir and Freundlich isotherm model constants for adsorption of BPB onto AFBP

Conc. (mg/l)	Langmuir isotherm				Freundlich isotherm		
	q_m (mg/g)	b	R_L	R^2	n	K_f (mg/g) (L/mg)$^{1/n}$	R^2
10.00	1.2092	0.6559	0.1323	0.9938	2.754	15.5382	0.9911
15.00	2.1730	0.5888	0.1017	0.9979	2.406	13.3844	0.9938
20.00	3.0684	0.5004	0.0908	0.9975	2.162	10.6170	0.9941
25.00	4.0933	0.4641	0.0794	0.9977	1.971	7.4955	0.9953
30.00	5.3079	0.4636	0.0671	0.9976	1.566	4.7973	0.9895

The correlation coefficients, (R^2) values of Langmuir and Freundlich isotherms are in the range of 0.9938-0.9979 and 0.9895-0.9953, (Table 2) respectively. These R^2 values described the fitness of the model for the set of data generated. The higher R^2 value indicates that Langmuir isotherm was a better fit for the adsorption of BPB than Freundlich isotherm.

The Freundlich the exponent (n), known as heterogeneity factor, is in range of 1.566-2.754, which falls within the ranges of 1 to 10 and this indicates favourability of the adsorption as well as advantageous adsorption [70]. Value of 'n' tending towards 10 displays a higher degree of homogeneity of the particle surface [71]. The lower value of 'n' signifies that the surface characteristics may be involve in the biosorption process more than a homogenous surface. The Langmuir model assumes monolayer coverage and constant adsorption energy while the Freundlich equation deals with heterogeneous

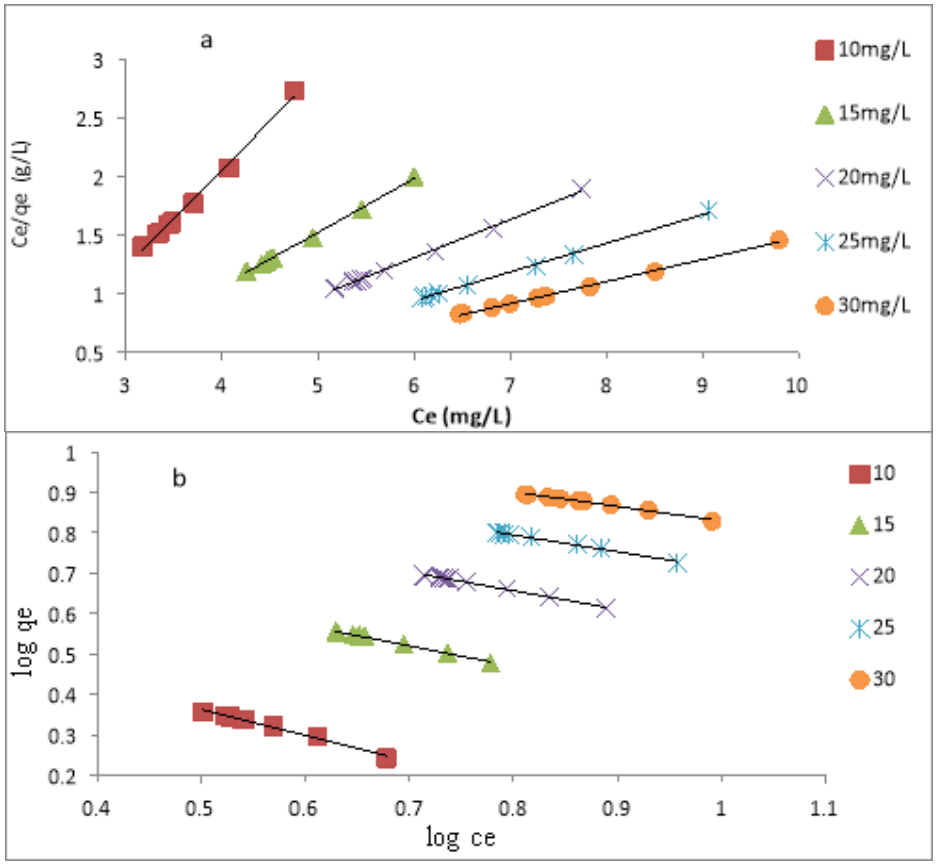

Fig. 7. (a) Langmuir and (b) Freundlich isotherm model plot for biosorption of BPB dye onto AFBP

surface adsorption. The applicability of both Langmuir and Freundlich isotherms to a studied system implies that both monolayer sorption and heterogeneous surface conditions occur under the experimental conditions used.

The essential characteristics of the Langmuir isotherms is described by a separation factor, R_L. The value R_L indicates the nature of the adsorption process [72]. The R_L for initial dye concentrations (10 to 30 mg/L) ranged from 0.1323 to 0.0671 and this indicates that biosorption of BPB onto AFBP is favorable. A similar range was reported by Pandimadevi, et al. [23], for the adsorption of methylene blue from aqueous solution onto activated carbon prepared from Flamboyant pods by chemical activation with H_2SO_4.

3.5 Kinetics of Study

The three common kinetic models applied to fit the experimental data obtained for BPB adsorption by AFBP are Pseudo first order (PFO), Pseudo second-order (PSO) and Elovich models.

3.5.1 Pseudo-first-order model

The intercepts and the slope of the plots of log (q_e–q_t) versus t (Fig. 8a) were used to determine the amount of BPB adsorbed onto AFBP at a different time q_t (mg/g), and the equilibrium (q_e). The values of k_1 were 0.0141, 0.0181, 0.0196, 0.0160, 0.0275 and 0.0122 min^{-1} for 5, 10, 15, 20, 25 and 30 mg/L while their corresponding q_e were 0.3980, 0.5944, 0.7077, 0.7960, 0.9789 and 0.8233 mg/g, respectively, (Table 3). The experimental equilibrium data ($q_{e(exp)}$) (0.7912-7.9970) were not close to the calculated equilibrium ($q_{e(cal)}$) (0.3980-0.8233) for the pseudo-first-order kinetics, as expected. The R^2 (0.7912, 0.7657, 0.7518, 0.6760, 0.8150, and 0.5931) of PFO are relatively low and thus suggest that this model cannot elucidate the adsorption process, due to the poor fitness of the adsorption data.

Table 3. The summary of the three common kinetic models applied to fit the experimental results of BPB adsorption by AFBP

Conc. mg/L	Pseudo first-order				pseudo second-order				Elovich		
	$q_{e\ (exp)}$ (mg/g)	K_1	$q_{e\ (cal)}$	R^2	$q_{e\ (cal)}$	$h= (k_2 q_e^2)$	K_2	R^2	α	β	R^2
5.00	0.7961	0.0141	0.3980	0.7912	0.8290	0.0545	0.0792	0.9962	0.1253	2.6224	0.8046
10.00	2.2769	0.0181	0.5944	0.7657	2.2999	0.5684	0.1075	0.9997	0.1341	11,068	0.8642
15.00	3.8190	0.0196	0.7077	0.7518	3.6075	1.3805	0.1061	0.9999	0.1576	3.7E+07	0.8702
20.00	4.9430	0.0160	0.7960	0.6760	4.9700	2.0576	0.0833	0.9999	0.2302	1.1E+07	0.8663
25.00	6.3051	0.0275	0.9789	0.8150	6.3530	3.8183	0.0946	1.0000	0.2657	1.2E+08	0.8306
30.00	7.8970	0.0122	0.8233	0.5931	7.8550	2.7778	0.0450	0.9997	0.2722	1.2E+10	0.8828

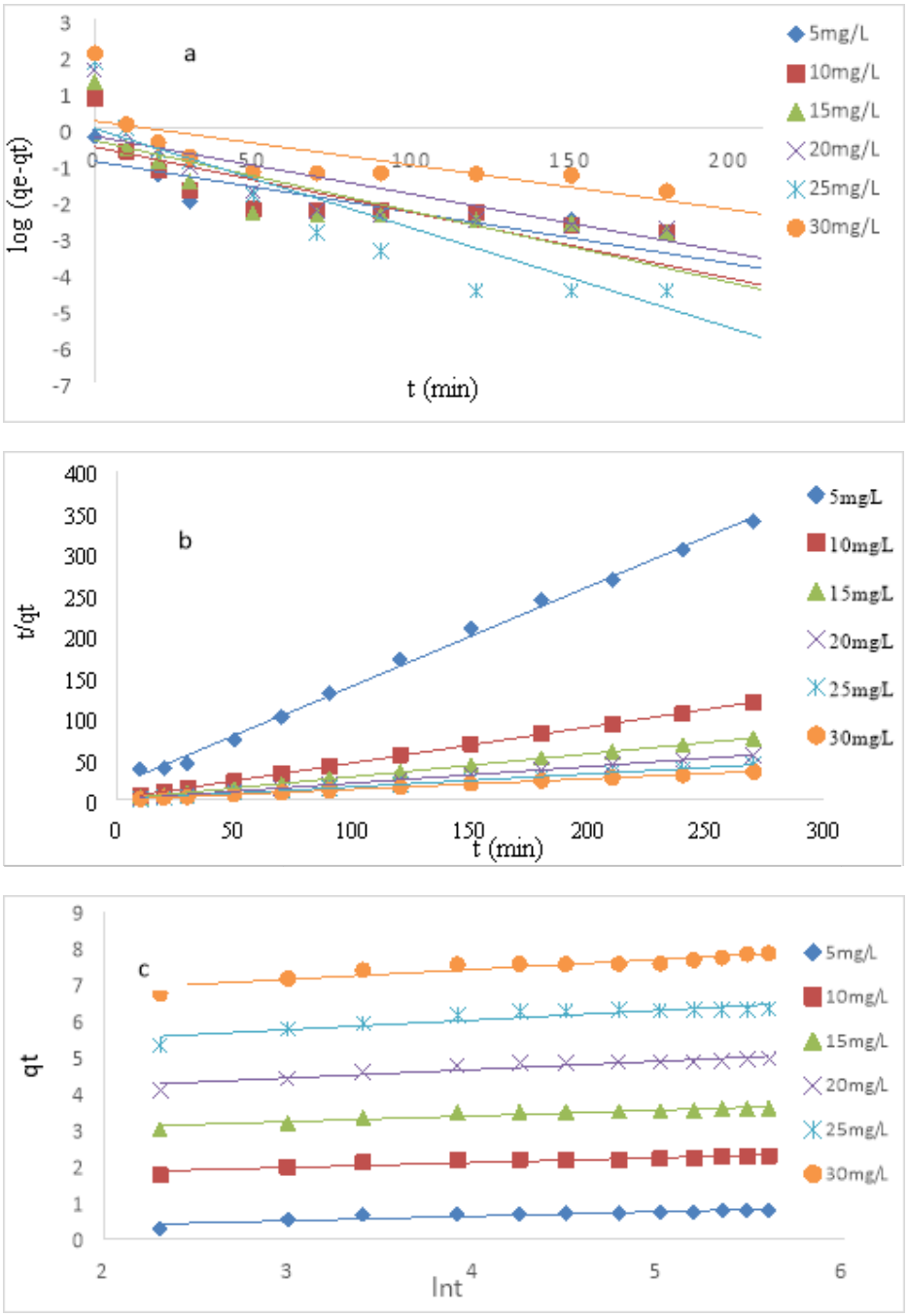

Fig. 8. Plot of (a) Pseudo-first-order, (b) pseudo-second-order and (c) Elovich kinetic model for the biosorption of BPB dye onto the AFBP

3.5.2 Pseudo-second-order model

The plot of t/q_t versus t (Fig. 8b) was used to evaluate the intercept ($1/k_2q_e^2$) and slope ($1/q_e$) of the pseudo-second-order (PSO) model equation. The values of model parameters (k_2, h, q_e and R^2) at different concentration were in the ranges of 0.0450-0.1075, 0.0545-3.8183, 0.8290-7.8550, and 0.9961-1.000, respectively. The values of R^2, h, and $q_{e(cal)}$ increased with increased BPB concentration but dropped for the last concentrations (30 mg/l) which may suggest

that desorption was about to set in at that condition. Similar kinetics was also observed in the adsorption of methylene blue and Congo red on papaya seeds [73] and *cattail* root [74], respectively.

3.5.3 Elovich model

The Elovich coefficients were evaluated from the plot of q_t versus ln t based on the experimental data (Fig. 8c). The values of α (initial adsorption rate) increased from 0.1253 to 0.2722 while the values of β (extent of surface characteristics coverage) increased from 2.6224 to $1.2x10^{10}$, as the concentration increased from 5 to 30 mg/l. The model's R^2 were 0.8046, 0.8642, 0.8702, 0.8663, 0.8306 and 0.8828 for 5, 10, 15, 20, 25 and 30 mg/L, respectively, and they are within the acceptable ranges (0.7500-1.000) suitable for biosorption kinetics [56]. However, these values were lower than the corresponding R^2 obtained for PFO and PSO, thus suggests that the Elovich model is not as suitable as expected for this study.

3.6 Test of Kinetic Models

The percentage sum of error squares (%SSE) and R^2 are used to determine the suitability of either PFO and PSO kinetic models for any adsorption system. Higher R^2 and lower %SSE suggest the goodness of the model fit for the experimental data, thus, data set with least %SSE is accepted for a given model [19]. %SSE obtained were in the ranges of 0.1585-50.0368 and 0.0005-0.0023 for the PFO and PSO, respectively. The calculated $q_{e(cal)}$ for PSO is closer to the experimental ($q_{e(exp)}$) and its %SSE value is lower compared to PFO. This substantiates further, that the PSO kinetic equation best describe the adsorption kinetics of BPB on the AFBP biosorbent. The order of fitness/suitability of the models, based on the R^2, is PSO > Elovich> PFO and this suggest that the adsorption is chemisorption.

4. CONCLUSION

Removal of bromophenol blue from dye aqueous solution was carried out using activated flamboyant pod biosorbent prepared from the agricultural residue (flamboyant pod) under the influence of various adsorption factors. The influence $ZnCl_2$, chemical activant, influenced the activation process as evident in the reduced ash content and adjusted functional groups on the surface of the flamboyant pod. Maximum adsorption capacity and removal efficiency obtained for 5-30 mg/L of BPB in the range of 0.79-7.89 mg/g and 47.80-8.42%, respectively. The two adsorption isotherms (Langmuir and Freundlich) isotherm explained the biosorption of BPB onto AFBP due to the heterogeneous and homogeneous surface characteristics of the adsorbent. The sorption kinetics of the system is well suited to pseudo-second-order at the expense of pseudo-first-order and Elovich kinetic models, while the order of fitness/suitability of the models is pseudo-second-order> Elovich> pseudo-first-order. Considering the data and analysis presented in this study, it suggests that flamboyant pod is promising biomass for the remediation of dye-bearing industrial effluents.

COMPETING INTERESTS

Authors have declared that no competing interests exist.

REFERENCES

1. Emenike PC, Omole DO, Ngene BU, Tenebe IT. Potentiality of agricultural adsorbent for the sequestering of metal ions. Global J. Environ. Sci. Manage. 2016;2(4):411-442.
2. Haffad H, Zbair M, Anfar Z, Ahsaine HA, Bouhlal H, Khallok H. Removal of reactive Red-198 dye using chitosan as an adsorbent: Optimization by central composite design coupled with response surface methodology. Tox. Reviews; 2019.
DOI: 10.1080/15569543.2019.1584822
3. Aghdasinia H, Asiabi HR. Adsorption of a cationic dye (methylene blue) by Iranian natural clays from aqueous solutions: Equilibrium, kinetic and thermodynamic study. Environ. Earth Sci. 2018;77:218-225.
4. Gedam VV, Raut P, Chahande A, Pathak P. Kinetic, thermodynamics and equilibrium studies on the removal of Congo red dye using activated teak leaf powder. Applied Wat. Sci. 2019;9:55-63.
5. Etim UJ, Umoren SA, Eduok UM. Coconut coir dust as a low cost adsorbent for the removal of cationic dye from aqueous solution. J. Saudi Chem. Soc. 2016;20(1): 67-76.
6. Choi H-J, Yu S-W. Biosorption of methylene blue from aqueous solution by agricultural bioadsorbent corncob. Environ. Eng. Res. 2019;24(1):99-106.

7. Kannanmarikani U, Sangareswari K, Rajarathinam K. Assessment of dyeing properties and quality parameters of natural dye extracted from *Lawsonia inermis*. Europ. J. Exp. Bio. 2015;5(7):62-70.
8. Swelam AA, Awad MB, Salem AM. Kinetics study on the removal of Cu(II) from aqueous solution using raw and modified pumpkin seed hulls-low cost biosorbents. Int. J. Environ. 2015;4(1):38-50.
9. Itodo AU, Oketunde FK. Activated carbon: Spent, regenerated and reuse for synthetic dyestuff effluent decolorization. Int. J. Env. Monit. Prot. 2017;4(4):29-37.
10. Rehman A, Ilyas S, Sultan S. Decolourization and degradation of azo dye, Synozol Red HF6BN, by *Pleurotus ostreatus*. Afr. J. Biotech. 2012;11(88): 15422-15429.
11. Donghee P, Yeoung-Sang Y, Jong MP. The past, present and future trends of biosorption. Biotech. Bioproc. Eng. 2010;15(1):86-102.
12. Aremu MO, Alade AO, Araromi DO, Bello A. Optimization of process parameters for the carbonization of flamboyant pod bark (*Delonix regia*). Europ. Sci. Jour. 2017;13(24):165-179.
13. Ramesh K, Rajappa A, Nandhakumar V. Adsorption of methylene blue onto microwave assisted zinc chloride activated carbon prepared from *Delonix regia* pods - isotherm and thermodynamic studies. Res. J. Chem. Sci. 2014;4(7):36-42.
14. Terdputtakun A, Arqueropanyo O, Sooksamiti P, Janhom S, Naksata W. Adsorption isotherm models and error analysis for single and binary adsorption of Cd(II) and Zn(II) using leonardite as adsorbent. Env. Earth Sci. 2017;76:777-787.
15. Massoudi FM, Etorki A. The use of peanut hull for the adsorption of colour from aqueous dye solutions and dye textile effluent. Orient. J. Chem. 2011;27(3):875-884.
16. Mane R, Bhusari VN. Removal of colour (dyes) from textile effluent by adsorption using orange and banana peel. Int. J. Eng. Res. Appl. 2011;2(3):1997-2004.
17. Hameed BH, Foo KY, Njoku VO. Microwave-assisted preparation of pumpkin seed hull activated carbon and its application for the adsorptive removal of 2,4-dichlorophenoxyacetic acid. The Chem. Eng. Jour. 2013;215-216:383–388.
18. Ncibi MC, Mohjoub B, Ouhaibi K. Valorisation of *Posidonia oceanica* leaf sheaths in removing synthetic dye from aqueous media using dynamic column system. Int. J. Environ. and Waste Manag. 2014;4:1-22.
19. Rajasulochana P, Preethy V. Comparison on efficiency of various techniques in treatment of waste and sewage water – A comprehensive review. Res.-Efficient Technol. 2016;2(4):175-184.
20. Alade AO, Amuda OS, Afolabi TJ, Okoya AA. Adsorption of naphthalene onto activated carbons derived from milk bush kernel shell and flamboyant pod. J. Environ. Chem. and Ecotoxico. 2012;4(7): 124-132.
21. Abulude FO, Adejayan AW. Nutritional values of flamboyant (*Delonix regia*) seeds obtained in Akure, Nigeria. Sci. and Edu. Develop. 2017;1(4):1-18.
22. Fahd K. Landscape plants: Manual of Srriyadh Plants. (Vol. 1). Saudi Arabia: High Commission for the development of Arriyadh; 2014.
23. Pandimadevi M, Rajalekshmi G, Mrithaa T, Viji CS. Preparation and characterisation of activated carbon from *Delonix regia* seeds for the removal of methylene blue dye. J. Indust. Poll. Contr. 2016;32(2):572-579.
24. Mithun M, Gangadware MV, Jadha V. Removal of methylene blue from wastewater by using *Delonix regia* seed powder as adsorbent. Int. J. Sci. Eng. and Techn. Res. 2016;5(6):2278–7798.
25. Adebisi SA, Amuda OS, Adejumo AL, Olayiwola AO, Farombi AG. Equilibrium, kinetic and thermodynamic studies of adsorption of aniline blue from aqueous media using steam-activated carbon prepared from *Delonix regia* pod. J. Wat. Res. Protect. 2015;7:1221-1233.
26. Syed S, Daniel S, Indhumathi P. Utilising the pods of *Delonix regia* activated carbon for the removal of mercury (II) by adsorption technique. Int. J. Res. Chem. Environ. 2013;3(1):60-65.
27. Owoyokun TO, Soile OO, Gayawan E. Chemometric analysis of the effects of initial concentrations, contact time and temperature on the adsorption capacity of Flamboyant tree (*Delonix regia*) pod. Int. J. Sci. Eng Res. 2013;4(3):1-10.
28. Sugumaran P, Priya SP, Ravichandran S. Production and characterization of

activated carbon from banana empty fruit bunch and *Delonix regia* fruit pod. J. Sustain. Energy Environ. 2012;3:125-132.

29. Jimoh OT, Iyaka AY, Nubaye M. Sorption study of Co (II), Cu(II), and Pb(II) ions removal from aqueous solution by adsorption on flamboyant flower (*Delonix regia*). Am. J. Chem. 2012;2(3):165-170.
30. Solairaj D, Palanivel R, Srinivasan P. Adsorption of methylene blue, bromophenol blue, and coomassie brilliant blue by α-Chitin nanoparticles. J. Adv. Res. 2015;27(1):1-11.
31. Okoye CC, Okey-Onyesolu CF, Chime DC, Achike CC. Adsorptive removal of bromophenol blue dye from aqueous solution using acid activated clay. Int. J. Sci. Res. Manage. 2018;6(3):2321-3418.
32. Ch A, Raju K, Satyanandam. Sorption of synthetic bromo phenol blue dye using *Gelidium cartilagineum* powder and optimization using central composite design. Int. J. Emerg. Eng. Res. Techn. 2015;3(12):109-127.
33. El-Dars F, Shalabi ME, Farag HA, Ibrahim HM, Abdelwahhab MZ. Adsorption kinetics of bromophenol blue and eriochrome black T using bentonite carbon composite material. Int. J. Sci. Eng. Res. 2015;6(5):1-14.
34. Mashkour MS. Decolorization of bromophenol blue dye under UV- radiation with ZnO as catalyst. Iraq. Nat. J. Chem. 2012;46:189-198.
35. Aadil A, Shahzad M, Kashif S, Muhammad M, Rabia A, Saba A. Comparative study of adsorptive removal of Congo red and brilliant green dyes from water using peanut shell. Middle-East J. Sci. Res. 2012;11(6):828-832.
36. Changying J, Talpur MA, Chandio FA, Junejo SA, Mari IA. Application of oven drying method on moisture content of ungrounded and grounded (long and short) rice for storage. J. Stored Prod. Postharvest Res. 2011;2(12):245-247.
37. Seshadri S, Sugumaran P, Priya SV, Ravichandran P. Production and characterization of activated carbon from banana empty fruit bunch and *Delonix regia* fruit pod. J. Sust. Energy Environ. 2012;3:125-132.
38. Jeandson C, Roberta N, Marcio AM, Dênia M. The oven-drying method for determination of water content in Brazil nut. Biosci. Journ. 2018;34(3):595-602.
39. Feng Y, Yang W, Chu W. Contribution of ash content related to methane adsorption behaviors of bituminous coals. Int. J. Chem. Eng. 2015;1:1-11.
40. Farah JY, El-Gendy NS. Performance, kinetics and equilibrium in biosorption of anionic dye acid Red 14 by the waste biomass of *Saccharomyces cerevisiae* as a low-cost biosorbent. Turk. J. of Eng. Environ. Sci. 2013;37:146-161.
41. Ibrahim MF, Abdelgadir AY. Effect of growth rate on fixed carbon, volatile matter and ash content of *Eucalyptus camaldulensis* wood of coppice origin grown in White Nile State, Sudan. J. Forest Prod. Indust. 2014;3(6):229-235.
42. Udoh AU, Duygu D, Ozer T, Akbulut A, Erkaya I, Yildiz K. Fourier transform infrared (FTIR) spectroscopy for identification of *Chlorella vulgaris* Beijerinck 1890 and *Scenedesmus obliquus* (Turpin) Kützing 1833. Afr. J. Biotech. 2012;11(16):3817-3824.
43. George ZK, Jie F, Kostas AM. New biosorbent materials: Selectivity and BioEng. Insights. Proces. 2014;2:419-440.
44. Quigley MN. Student preparation of standard solutions. J. Chem. Edu. 2011;68(6):505-509.
45. Nguyen VT, Tran TH. Application of chitosan solutions for rice production in Vietnam. Afr. J. Biotech. 2013;12(4):382-384.
46. Altaher H. Preliminary study of the effect of using biosorbents on the pollution of the treated water. Glob. NEST Jour. 2014;16(10):1-10.
47. Sen TK. Review on dye removal from its aqueous solution into alternative cost effective and non-conventional adsorbents. J. Chem. Proc. Eng. 2014;1:1-11.
48. Zeroual Y, Kim BS, Kim CS, Blaghen M, Lee KM. Biosorption of bromophenol blue from aqueous solutions by *Rhizopus stolonifer* biomass. Wat. Air, and Soil Poll. 2016;1(4):135-146.
49. Hasan S, Fuat G, Gülbahar AS. Using grape pulp as a new alternative biosorbent for removal of a model basic dye. Asia-Pac. J. of Chem. Eng. 2014;9(2):1-10.
50. Alabi O, Alade AO, Afolabi TJ. Process optimization of adsorption of Cr(VI) on adsorbent prepared from *Bauhinia rufescens* pod by Box-Behnken Design, Sep. Sci. Technol; 2019.
51. Thitame PV, Shukla SR. Adsorptive removal of reactive dyes from aqueous

solution using activated carbon synthesized from waste biomass materials. Int. J. Environ. Sci. Technol. 2016;13:561–570.
52. Inyinbor AA, Adekola FA, Olatunji GA. Adsorption of Rhodamine B dye from aqueous solution on *Irvingia gabonensis* biomass: Kinetics and thermodynamics studies. South. Afr. J. Chem. 2015;68:115-125.
53. Feng-Chin W, Ru-Ling T, Ruey-Shin J. Characteristics of elovich equation used for the analysis of adsorption kinetics in dye-chitosan systems. Che. Eng. J. 2009;150(2-3):366-373.
54. Idris S, Iyaka YA, Ndamitso MM, Mohammed EB, Umar MT. Evaluation of kinetic models of copper and lead uptake from dye wastewater by activated pride of Barbados shell. Am. J. Chem. 2011;1(2): 47-51.
55. Hesas RH, Wan Daud WA, Sahu JN, Arami NA. Preparation and characterization of activated carbon from apple waste by microwave assisted phosphoric acid activation. Bio Resourc. 2013;8(2):2950-2966.
56. Ponnusami V, Sunil K, Gunasekar V. Removal of methylene blue from aqueous effuent using fixed bed of groundnut shell powder. J. Chem. 2013;1-5.
57. Yusoff MS, Mohammadizaroun M. Review on landfill leachate and wastewater treatment using physical-chemical techniques: Their performance and limitations. Int. J. Curr. Lif. Sci. 2014;4(12):12068-12074.
58. Senthilkumaar S, Krishna SK, Kalaamani P, Subburamaan CV, Ganapathi S. Adsorption of organophosphorous pesticide from aqueous solution using waste jute fiber carbon. Mod. Appl. Sci. 2010;4(6):422-434.
59. Murali K, Uma RN. Removal of basic dye (Methylene Blue) using low cost biosorbent: Water hyacinth. Int. J. Adv. Eng. Technol. 2012;1-15.
60. Bello OS, Auta M, Ayodele OB. Ackee apple (*Blighia sapida*) seeds: A novel adsorbent for the removal of Congo Red dye from aqueous solutions. Chem. Ecol. 2012;29(1):23-35.
61. Asma N, Hizbullah K, Amir S, Zakaria M, Nawshad M, Muhammad IK. Potential biosorbent derived from Calligonum polygonoides for removal of methylene blue dye from aqueous solution. Sci. Worl. Jour. 2015;1:1-11.
62. Jeyabalan T, Praveen P. Degradation of dyes (Methylene Blue and Congo Red Dye) using phosphomolybdic acid. Int J. Sci. Res. 2012;3:2319-7064.
63. Nimkar DA, Chavan SK. Removal of Congo red dye from aqueous solution by using saw dust as an adsorbent. Int. J. of Eng. Res. Applic. 2014;4(4):47-51.
64. Khalifa R, Safa C, Béchir BT. Adsorption of methylene blue dye onto Aleppo pine (*Pinus halepensis* Mill.) fibers: A kinetic modeling studies. Elix. Chem. Eng. 2016;97:42317-42322.
65. Salman JM, Amrin AR, Hassan MH, Jouda SA. Removal of Congo red dye from aqueous solution by using natural materials. Mesop. Env. Jour. 2015;1(3):82-89.
66. Asfaram A, Fathi MR, Saeid K, Naraki M. Removal of direct Red 12B by garlic peel as a cheap adsorbent: Kinetics, thermodynamic and equilibrium isotherms study of removal. Spectr. Acta Part A Molec. Biomolec. Spectr. 2014;127(2):415-421.
67. Wanyonyi WC, Onyari JM, Shiundu P. Adsorption of Congo red dye from aqueous solutions using roots of *Eichhornia crassipes*: Kinetic and equilibrium studies. Energy Procedia. 2014;50:862–869.
68. Ali A, Kovo A, Adetunji S. Methylene blue, and brilliant green dyes removal from aqueous solution using agricultural wastes activated carbon. J. of Encapsul. Adsorp. Sci. 2017;7:95-107.
69. Kim DS, Se-Jin O, Ijagbemi CO, Baek MH. Removal of malachite green from aqueous solution using degreased coffee bean. J. Hazard. Mater. 2010;176(1-3):820–828.
70. Adebayo GB, Adegoke HI, Jamiu W, Balogun BB, Jimoh AA. Adsorption of Mn(II) and Co(II) ions from aqueous solution using maize cob activated carbon: Kinetics and thermodynamics studies. J. Appl. Sci. Env. Man. 2015;19(4):737-748.
71. Ramachandra TV, Ahalya N, Kanamadi RD. Biosorption: Techniques and mechanisms. CES Tech. Rep. 2013;110.
72. Mohammad SA, Rexona K, Mohammad AR. Removal of Congo red dye from industrial wastewater by untreated sawdust. Am. J. Environ. Protect. 2015; 4(5):207-213.

73. Hameed BH. Evaluation of papaya seeds as a novel non-conventional low-cost adsorbent for removal of methylene blue. J. Hazard. Matter. 2009;162(2-3):939-944.

74. Hu Z, Chen H, Ji F, Yuan S. Removal of Congo red from aqueous solution by cattail root. J. Haz. Mat. 2010;1(3):292-297.

Peer-review history:
The peer review history for this paper can be accessed here:
http://www.sdiarticle4.com/review-history/58808